

Nonstandard interactions of tau neutrino via charged Higgs and W' contribution

Ahmed Rashed ^{†‡ 1}, Murugeswaran Duraisamy ^{† 2} and Alakabha Datta ^{† 3}

[†] *Department of Physics and Astronomy,
University of Mississippi,
Lewis Hall, University, Mississippi, 38677 USA*

[‡] *Department of Physics, Faculty of Science,
Ain Shams University, Cairo, 11566, Egypt*

(December 2, 2024)

Abstract

We consider charged Higgs and W' gauge boson contributions to the quasielastic scattering $\nu_\tau + n \rightarrow \tau^- + p$ and $\bar{\nu}_\tau + p \rightarrow \tau^+ + n$. These effects modify the standard model cross section for these processes and thus impact the extraction of the neutrino mixing angles θ_{23} and θ_{13} . We include form factor effects in our calculations and find the deviation of the actual mixing angle from the measured one, assuming the standard model cross section, can be significant and can depend on the energy of the neutrino.

¹E-mail: amrashed@phy.olemiss.edu

²E-mail: duraism@phy.olemiss.edu

³E-mail: datta@phy.olemiss.edu

1 Introduction

We now know that neutrinos have masses and that there is a leptonic mixing matrix just as there is a quark mixing matrix. This fact has been firmly established through a variety of solar, atmospheric, and terrestrial neutrino oscillation experiments. The next phase in the neutrino physics program is the precision measurement of the mixing angles, finding evidence for CP violation and measuring the absolute masses to resolve the mass hierarchy problem.

The existence of neutrino masses and mixing requires physics beyond the standard model (SM). Hence it is not unexpected that neutrinos could have non-standard interactions (NSI). The effects of NSI have been widely considered in neutrino phenomenology [1, 2, 3, 4, 5, 6, 7, 8, 9, 10, 11, 12, 13, 14, 15, 16, 17, 18, 19, 20, 21, 22, 23, 24, 25, 26, 27, 28, 29, 30, 31, 32].

It has been established that NSI cannot be an explanation for the standard oscillation phenomena, but it may be present as a subleading effect. Many NSI involve flavor changing neutral current or charged current lepton flavor violating processes. In this paper we consider charged current interactions involving a charged Higgs and a W' gauge boson in the quasielastic scattering processes $\nu_\tau + n \rightarrow \tau^- + p$ and $\bar{\nu}_\tau + p \rightarrow \tau^+ + n$. In neutrino experiments, to measure the mixing angle the neutrino-nucleus interaction is assumed to be SM-like. If there is a charged Higgs or a W' contribution to this interaction, then there will be an error in the extracted mixing angle. We will calculate the error in the extracted mixing angle.

The reaction $\nu_\tau + n \rightarrow \tau^- + p$ is relevant for experiments like Super-Kamiokande (Super-K) [33, 34] and OPERA [35] that seek to measure $\nu_\mu \rightarrow \nu_\tau$ oscillation by the observation of the τ lepton. The above interaction is also important for the DONuT experiment [36] which measured the charged-current (CC) interaction cross section of the tau neutrino. The DONuT central-value results for a ν_τ scattering cross section show deviation from the standard model predictions by about 40% but with large experimental errors; thus, the measurements are consistent with the standard model. The new physics (NP) effects calculated in this paper modify the SM cross sections by less than 10% and are therefore consistent with the DONuT measurements. There have been recent measurements of the appearance of atmospheric tau neutrinos by Super-K [33] and by the OPERA Collaboration [35].

The reactor neutrino experiments such as Double Chooz [37], Daya Bay [38], and RENO [39] measure the mixing angle θ_{13} from the survival probability of an electron antineutrino, $P(\bar{\nu}_e \rightarrow \bar{\nu}_e)$. If these experiments are designed to observe $\bar{\nu}_e \rightarrow \bar{\nu}_\tau$ oscillation, the scattering process $\bar{\nu}_\tau + p \rightarrow \tau^+ + n$ will be important. The two processes $\nu_\tau + n \rightarrow \tau^- + p$ and $\bar{\nu}_\tau + p \rightarrow \tau^+ + n$ involve the same new physics (NP) operators.

Generally, neutrino scattering contains contributions from various processes such as quasielastic scattering (QE), resonance scattering (RES), and deep inelastic scattering (DIS). Just above the threshold energy for τ production, which is 3.45 GeV [33, 34], the quasielastic interaction dominates in ν_τ scattering [40, 41]. At

higher scattering energies other processes have to be included. For instance, the DIS is expected to be dominant above around 10 GeV [41], and so ν_τ scattering at the OPERA experiment, running at the average neutrino energy $E_\nu = 17$ GeV [35], will be dominated by DIS. In this paper we will study the effects of NSI only in QE scattering, so we will limit ourselves to energies where QE is dominant. A full NSI analysis including all processes in ν_τ scattering will be discussed in Ref. [42].

There are several reasons to consider NSI involving the (ν_τ, τ) sector. First, the third generation may be more sensitive to new physics effects because of their larger masses. As an example, in certain versions of the two Higgs doublet models (2HDM) the couplings of the new Higgs bosons are proportional to the masses, and so new physics effects are more pronounced for the third generation. Second, the constraints on NP involving the third generation leptons are somewhat weaker, allowing for larger new physics effects. Interestingly, the branching ratio of B decays to τ final states shows some tension with the SM predictions [43, 44] and this could indicate NP, possibly in the scalar or gauge boson sector [45]. Some examples of work that deals with NSI at the detector, though not necessarily involving the third family leptons, can be found in Refs. [46, 47, 48].

If there is NP involving the third generation leptons, one can search for it in B decays such as $B \rightarrow \tau \nu_\tau$, $B \rightarrow D^{(*)} \tau \nu_\tau$ [49], $b \rightarrow s \tau^+ \tau^-$ etc. In general, the NP interaction in B decays may not be related to the one in $\nu_\tau + n \rightarrow \tau^- + p$ and $\bar{\nu}_\tau + p \rightarrow \tau^+ + n$, and so these scattering processes probe different NP. The same NP in $\nu_\tau + n \rightarrow \tau^- + p$ and $\bar{\nu}_\tau + p \rightarrow \tau^+ + n$ can be probed in τ decays [50], and we will consider the constraint on NP from this decay. However, in general, the scattering and the decay processes probe NP in different energy regions.

The form of NP in $\nu_\tau + n \rightarrow \tau^- + p$ involves the operator $\mathcal{O}_{NP} = \bar{u} \Gamma_i d \bar{\tau} \Gamma_j \nu_\tau$, where $\Gamma_{i,j}$ are some Dirac structures. The process $\bar{\nu}_\tau + p \rightarrow \tau^+ + n$ gets a contribution from \mathcal{O}_{NP}^\dagger . We will assume CP conserving NP in this paper, and so the coefficients of the NP operators are real. The same NP operator can also contribute to hadronic tau decays $\tau^- \rightarrow \pi^- \nu_\tau$ and $\tau^- \rightarrow \rho^- \nu_\tau$, and the measured branching ratio of these decays can be used to constrain the couplings in the operator \mathcal{O}_{NP} . The ratio of the charged Higgs contribution to the SM in $\nu_\tau + n \rightarrow \tau^- + p$ and $\bar{\nu}_\tau + p \rightarrow \tau^+ + n$ is roughly (m_N/m_π) larger compared to the same ratio in $\tau^- \rightarrow \pi^- \nu_\tau$, where $m_{N,\pi}$ are the nucleon and pion masses. Hence, significant charged Higgs effects are possible in $\nu_\tau + n \rightarrow \tau^- + p$ and $\bar{\nu}_\tau + p \rightarrow \tau^+ + n$ even after imposing constraints from τ decays. We note that new interactions in the up and down quark sectors can be constrained if one assumes CKM unitarity. However, we do not consider this constraint as the NP in \mathcal{O}_{NP} involves contributions from both the quark and the lepton sectors.

As noted above, at the quark level NSI in $\nu_\tau + n \rightarrow \tau^- + p$ and $\bar{\nu}_\tau + p \rightarrow \tau^+ + n$ involve the u and the d quarks. Often in the analysis of NSI, hadronization effects of the quarks via form factors are not included. As we show in our calculation the form factors play an important role in the energy dependence of the NP effects. In an accurate analysis one should also include nuclear physics effects which take into

account the fact that the neutron and the proton are not free but bound in the nucleus. There is a certain amount of model dependence in this part of the analysis [51], and therefore we will not include nuclear effects in our calculation. Such effects can be easily incorporated once the free scattering cross sections are known.

The paper is organized in the following way. In the next section, we present a model-independent analysis of NP effects. In the following three sections, we consider the neutrino and antineutrino quasielastic scattering in the SM, in a model with charged Higgs and in a model with an extra W' gauge boson. In the last section, we present our conclusions.

2 Model-independent analysis of new physics

The process $\nu_\tau + n \rightarrow \tau^- + p$ will impact the measurement of the oscillation probability for the $\nu_\mu \rightarrow \nu_\tau$ transition and hence the extraction of the mixing angle θ_{23} . The measurement of the atmospheric mixing angle θ_{23} relies on the following relationship [52]:

$$N(\nu_\tau) = P(\nu_\mu \rightarrow \nu_\tau) \times \Phi(\nu_\mu) \times \sigma_{\text{SM}}(\nu_\tau), \quad (1)$$

where $N(\nu_\tau)$ is the number of observed events, $\Phi(\nu_\mu)$ is the flux of muon neutrinos at the detector, $\sigma^{\text{SM}}(\nu_\tau)$ is the total cross section of tau neutrino interactions with nucleons in the SM at the detector, and $P(\nu_\mu \rightarrow \nu_\tau)$ is the probability for the flavor transition $\nu_\mu \rightarrow \nu_\tau$. This probability is a function of $(E, L, \Delta m_{ij}^2, \theta_{ij})$ with $i, j = 1, 2, 3$, where Δm_{ij}^2 is the squared-mass difference, θ_{ij} is the mixing angle, E is the energy of neutrinos, and L is the distance traveled by neutrinos. The dominant term of the probability is

$$P(\nu_\mu \rightarrow \nu_\tau) \approx \sin^2 2\theta_{23} \cos^4 \theta_{13} \sin^2(\Delta m_{23}^2 L/4E). \quad (2)$$

In the presence of NP, Eq. 1 is modified as

$$N(\nu_\tau) = P(\nu_\mu \rightarrow \nu_\tau) \times \Phi(\nu_\mu) \times \sigma_{\text{tot}}(\nu_\tau), \quad (3)$$

with $\sigma_{\text{tot}}(\nu_\tau) = \sigma_{\text{SM}}(\nu_\tau) + \sigma_{\text{NP}}(\nu_\tau)$, where $\sigma_{\text{NP}}(\nu_\tau)$ refers to the additional terms of the SM contribution towards the total cross section. Hence, $\sigma_{\text{NP}}(\nu_\tau)$ includes contributions from both the SM and NP interference amplitudes, and the pure NP amplitude. From Eqs. (1, 3), assuming θ_{13} to be small,⁴

$$\sin^2 2(\theta_{23}) = \sin^2 2(\theta_{23})_{\text{SM}} \frac{1}{1 + r_{23}}, \quad (4)$$

where $\theta_{23} = (\theta_{23})_{\text{SM}} + \delta_{23}$ is the actual atmospheric mixing angle, whereas $(\theta_{23})_{\text{SM}}$ is the extracted mixing angle assuming the SM ν_τ scattering cross section. Here

⁴The presence of NP impacts the extraction of the combination $\sin^2 2\theta_{23} \cos^4 \theta_{13}$. The NP changes the extracted value of θ_{23} as well as θ_{13} . But we fix the value of θ_{13} as an input at this point.

$r_{23} = \sigma_{NP}(\nu_\tau)/\sigma_{SM}(\nu_\tau)$ is the ratio between the NP contribution, including the pure NP and interference terms, to the SM cross section. This means that r_{23} can be positive or negative. Assuming negligible new physics effects in the $\mu - N$ interaction, the actual mixing angle θ_{23} is the same as the mixing angle extracted from the survival probability $P(\nu_\mu \rightarrow \nu_\mu)$ measurement. We will take the best-fit value for the mixing angle to be given by $\theta_{23} = 42.8^\circ$ [53]. In other words, the presence of new physics in a ν_τ -nucleon scattering will result in the mixing angle, extracted from a ν_τ appearance experiment, being different than the mixing angle from ν_μ survival probability measurements. The relationship between the ratio r_{23} and δ_{23} can be expressed in a model-independent form as

$$r_{23} = \left[\frac{\sin 2(\theta_{23})_{SM}}{\sin 2((\theta_{23})_{SM} + \delta_{23})} \right]^2 - 1. \quad (5)$$

The reactor neutrino experiments can determine the mixing angle θ_{13} from the oscillation probability, $P(\bar{\nu}_e \rightarrow \bar{\nu}_e)$. The probability of the tau antineutrino appearance $\bar{\nu}_e \rightarrow \bar{\nu}_\tau$ can be used to extract θ_{13} . In this case the effect of NP contributions to the process $\bar{\nu}_\tau + p \rightarrow \tau^+ + n$ is pertinent. The relationship used in measuring θ_{13} will be given as

$$N(\bar{\nu}_\tau) = P(\bar{\nu}_e \rightarrow \bar{\nu}_\tau) \times \Phi(\bar{\nu}_e) \times \sigma_{\text{tot}}(\bar{\nu}_\tau), \quad (6)$$

where [54, 55, 56]

$$P(\bar{\nu}_e \rightarrow \bar{\nu}_\tau) \approx \sin^2 2\theta_{13} \cos^2 \theta_{23} \sin^2(\Delta m_{13}^2 L/4E). \quad (7)$$

Thus the relationship between the ratio of the NP contribution to the SM cross section $r_{13} = \sigma_{NP}(\bar{\nu}_\tau)/\sigma_{SM}(\bar{\nu}_\tau)$, which can be positive or negative, and δ_{13} can be obtained in a model-independent form as

$$r_{13} = \left[\frac{\sin 2(\theta_{13})_{SM}}{\sin 2((\theta_{13})_{SM} + \delta_{13})} \right]^2 - 1. \quad (8)$$

In Fig. 1 we show the correlation between $r_{23(13)}\%$ and $\delta_{23(13)}$ [Deg]. One can see that $\delta_{23} \sim -5^\circ$ requires $r_{23} \sim 5\%$. But $\delta_{13} \sim -1^\circ$ requires $r_{13} \sim 25\%$. In the following sections, we consider specific models of NP to calculate r_{23} and r_{13} . We will consider a model with a charged Higgs and a W' model with both left- and right-handed couplings.

3 Quasielastic neutrino scattering off free nucleon – the SM

In this section we consider the SM contribution to $\nu_\tau + n \rightarrow \tau^- + p$ and $\bar{\nu}_\tau + p \rightarrow \tau^+ + n$. We first summarize the SM results for the quasielastic scattering of a neutrino on a free neutron target,

$$\nu_l(k) + n(p) \rightarrow l^-(k') + p(p'), \quad (9)$$

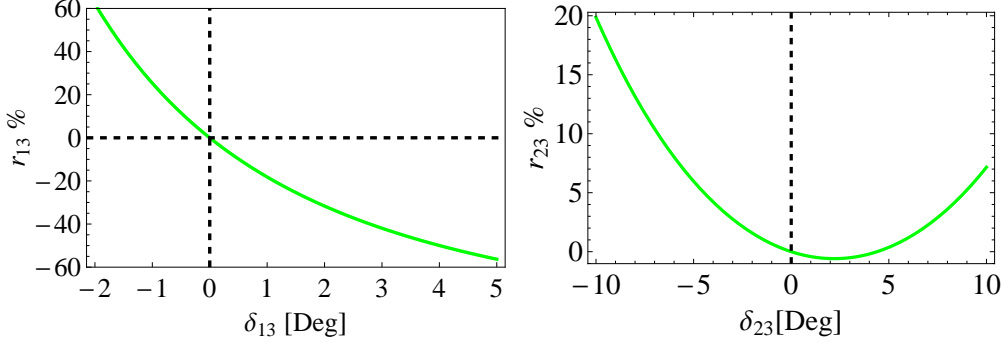


Figure 1: Correlation plot for $r_{23} = \sigma_{NP}(\nu_\tau)/\sigma_{SM}(\nu_\tau)\%$ versus $\delta_{23}[Deg]$, and $r_{13} = \sigma_{NP}(\bar{\nu}_\tau)/\sigma_{SM}(\bar{\nu}_\tau)\%$ versus $\delta_{13}[Deg]$.

where k, k', p , and p' denote the four-momenta and l indicates the lepton e, μ , or τ . The spin-averaged matrix element squared for the above reaction is a convolution of spin-averaged leptonic and hadronic tensors $L^{\mu\nu}$ and $H^{\mu\nu}$:

$$|\bar{\mathcal{M}}|^2 = \frac{G_F^2}{2} L^{\mu\nu} H_{\mu\nu}. \quad (10)$$

The leptonic tensor calculation is straightforward, but the hadronic tensor involves nonperturbative effects. In order to calculate the hadronic tensor, we define the charged hadronic current for this process:

$$\begin{aligned} \langle p(p') | J_\mu^+ | n(p) \rangle &= V_{ud} \langle p(p') | (V_\mu - A_\mu) | n(p) \rangle \\ &= V_{ud} \bar{p}(p') \Gamma_\mu n(p). \end{aligned} \quad (11)$$

The expressions for the matrix elements of the vector and axial-vector currents are summarized in terms of six form factors in the Appendix. Due to time reversal invariance, the form factors are real functions of $t = q^2$. When invariance under charge conjugation holds, two form factors vanish ($F_S = 0, F_T = 0$) [57]. The matrix element, then, can be written as

$$\begin{aligned} \mathcal{M} &= \frac{G_F \cos \theta_c}{\sqrt{2}} \bar{u}_l(k') \gamma^\mu (1 - \gamma_5) u_{\nu_l}(k) \\ &\quad \bar{u}_{N'}(p') \left[F_1^V(t) \gamma_\mu + F_2^V(t) i \frac{\sigma_{\mu\nu} q^\nu}{2M} + F_A(t) \gamma_\mu \gamma_5 + F_P(t) \gamma_5 \frac{q_\mu}{M} \right] u_N(p), \end{aligned} \quad (12)$$

where N and N' are the initial and final nucleons, while l and ν_l are the final charged lepton and the initial neutrino. In our case $N = n, N' = p, l = \tau$, and $\nu_l = \nu_\tau$.

After evaluating $|\bar{\mathcal{M}}|^2$, one can obtain the SM differential cross section for the reaction in Eq. (9) [57],

$$\frac{d\sigma_{SM}(\nu_l)}{dt} = \frac{M^2 G_F^2 \cos^2 \theta_c}{8\pi E_\nu^2} \left[A_{SM} + B_{SM} \frac{(s-u)}{M^2} + C_{SM} \frac{(s-u)^2}{M^4} \right], \quad (13)$$

where $G_F = 1.16637 \times 10^{-5} \text{ GeV}^{-2}$ is the Fermi coupling constant, $\cos \theta_c = 0.9746$ is the cosine of the Cabibbo angle, M_W is the W boson mass, and E_ν is the incident neutrino energy. $M = (M_p + M_n)/2 \approx 938.9 \text{ MeV}$ is the nucleon mass, and we neglect the proton-neutron mass difference. The expressions for the coefficients f_{SM} ($f = A, B, C$) are summarized in the Appendix. The Mandelstam variables are defined by $s = (k + p)^2$, $t = q^2 = (k - k')^2$, and $u = (k - p')^2$. The expressions for these variables in terms of E_ν and the lepton energy E_l are given in the Appendix.

The quasielastic scattering of an antineutrino on a free nucleon is given by

$$\bar{\nu}_l(k) + p(p) \rightarrow l^+(k') + n(p'). \quad (14)$$

The charged hadronic current becomes [40, 58]

$$\begin{aligned} \langle n(p') | J_\mu^- | p(p) \rangle &= \langle p(p) | J_\mu^+ | n(p') \rangle^\dagger \\ &= V_{ud} \bar{n}(p') \tilde{\Gamma}_\mu p(p), \end{aligned} \quad (15)$$

where

$$\tilde{\Gamma}_\mu(p, p') = \gamma_0 \Gamma_\mu^\dagger(p', p) \gamma_0. \quad (16)$$

The relationship between the differential cross sections of $\nu_\tau + n \rightarrow \tau^- + p$ and $\bar{\nu}_\tau + p \rightarrow \tau^+ + n$ is [58, 59]

$$\frac{d\sigma_{SM}(\nu_l)}{dt}(s, t, u) = \frac{d\sigma_{SM}(\bar{\nu}_l)}{dt}(u, t, s). \quad (17)$$

Thus, the matrix element is given by Eq. 12, and the differential cross section, similarly to Eq. 13, is given by

$$\frac{d\sigma_{SM}(\bar{\nu}_l)}{dt} = \frac{M^2 G_F^2 \cos^2 \theta_c}{8\pi E_\nu^2} \left[A_{SM} - B_{SM} \frac{(s - u)}{M^2} + C_{SM} \frac{(s - u)^2}{M^4} \right]. \quad (18)$$

The negative sign of B_{SM} leads to a relatively smaller cross section for the antineutrino scattering.

4 Quasielastic neutrino scattering off free nucleon – Charged Higgs Effect

We consider here the charged Higgs contribution to $\nu_\tau + n \rightarrow \tau^- + p$ and $\bar{\nu}_\tau + p \rightarrow \tau^+ + n$. Charged Higgs particles appear in multi-Higgs models. In the SM the Higgs couples to the fermion masses, but in a general multi-Higgs model the charged Higgs may not couple to the mass. What is true in most models is that the coupling of the charged Higgs to the leptons is no longer universal. Hence, the extraction of θ_{23} and θ_{13} from $\nu_\mu \rightarrow \nu_\mu$ and $\bar{\nu}_e \rightarrow \bar{\nu}_e$ survival probabilities, respectively, will be different

from $\nu_\mu \rightarrow \nu_\tau$ and $\bar{\nu}_e \rightarrow \bar{\nu}_\tau$ probabilities, respectively, in the presence of a charged Higgs effect.

The most general coupling of the charged Higgs is

$$\mathcal{L} = \frac{g}{2\sqrt{2}} \left[V_{u_i d_j} \bar{u}_i (g_S^{u_i d_j} \pm g_P^{u_i d_j} \gamma^5) d_j + \bar{\nu}_i (g_S^{\nu_i l_j} \pm g_P^{\nu_i l_j} \gamma^5) l_j \right] H^\pm, \quad (19)$$

where u_i and d_j refer to up and down type quarks, and ν_i and l_j refer to neutrinos and charged leptons. The other parameters are as follows: $g = e/\sin\theta_W$ is the SM weak coupling constant, $V_{u_i d_j}$ is the CKM matrix element, and $g_{S,P}$ are the scalar and pseudoscalar couplings of the charged Higgs to fermions. Here, in this work, we assume the couplings $g_{S,P}$ are real.

We will choose the couplings $g_{S,P}$, relevant for $\nu_\tau + n \rightarrow \tau^- + p$ and $\bar{\nu}_\tau + p \rightarrow \tau^+ + n$, to be given by the two Higgs doublet model of type II (2HDM II). In the 2HDM II these couplings are related to couplings in other sectors and so can be constrained by measurements in these other sectors. However, in our analysis, to keep things general we will not assume any relation between the couplings $g_{S,P}$ and the couplings in other sectors, thereby avoiding constraints from other sectors. To constrain the couplings $g_{S,P}$ we will only consider processes that are generated by $\mathcal{O}_{NP} = \bar{u}\Gamma_i d \bar{\tau}\Gamma_j \nu_\tau$. In the 2HDM II, constraints on the model parameters come from various sectors [60]. These constraints turn out to be similar but slightly stronger than the ones obtained in our analysis.

The coupling of charged Higgs boson (H^\pm) interactions to a SM fermion in the 2HDM II is [61]

$$\mathcal{L} = \frac{g}{\sqrt{2}M_W} \sum_{ij} \left[m_{u_i} \cot\beta \bar{u}_i V_{ij} P_{L,R} d_j + m_{d_j} \tan\beta \bar{u}_i V_{ij} P_{R,L} d_j + m_{l_j} \tan\beta \bar{\nu}_i P_{R,L} l_j \right] H^\pm, \quad (20)$$

where $P_{L,R} = (1 \mp \gamma^5)/2$, and $\tan\beta$ is the ratio between the two vacuum expectation values (vev's) of the two Higgs doublets. Comparing Eq. (19) and Eq. (20), one can obtain

$$\begin{aligned} g_S^{u_i d_j} &= \left(\frac{m_{d_j} \tan\beta + m_{u_i} \cot\beta}{M_W} \right), \\ g_P^{u_i d_j} &= \left(\frac{m_{d_j} \tan\beta - m_{u_i} \cot\beta}{M_W} \right), \\ g_S^{\nu_i l_j} &= g_P^{\nu_i l_j} = \frac{m_{l_j} \tan\beta}{M_W}. \end{aligned} \quad (21)$$

Constraints on the size of the operator $\mathcal{O}_{NP} = \bar{u}\Gamma_i d \bar{\tau}\Gamma_j \nu_\tau$ can be obtained from the branching ratio of the decay $\tau^- \rightarrow \pi^- \nu_\tau$. In the presence of a charged Higgs, the branching ratio for this process is

$$Br_{\tau^- \rightarrow \pi^- \nu_\tau}^{SM+H} = Br_{\tau^- \rightarrow \pi^- \nu_\tau}^{SM} (1 + r_H^2), \quad (22)$$

where the charged Higgs contribution is

$$r_H^\pi = \left(\frac{m_u - m_d \tan^2 \beta}{m_u + m_d} \right) \frac{m_\pi^2}{m_H^2}. \quad (23)$$

The SM branching ratio is related to the tau lepton width (Γ_τ) and the decay rate($\Gamma_{\tau^- \rightarrow \pi^- \nu_\tau}^{SM}$) as $Br_{\tau^- \rightarrow \pi^- \nu_\tau}^{SM} = \Gamma_{\tau^- \rightarrow \pi^- \nu_\tau}^{SM} / \Gamma_\tau$ with

$$\Gamma_{\tau^- \rightarrow \pi^- \nu_\tau}^{SM} = \frac{G_F^2}{16\pi} |V_{ud}|^2 f_\pi^2 m_\tau^3 \left(1 - \frac{m_\pi^2}{m_\tau^2} \right)^2 \delta_{\tau/\pi}. \quad (24)$$

Here $\delta_{\tau/\pi} = 1.0016 \pm 0.0014$ [62] is the radiative correction. Further, the SM branching ratio can also be expressed as [63]

$$Br_{\tau^- \rightarrow \pi^- \nu_\tau}^{SM} = 0.607 Br(\tau^- \rightarrow \nu_\tau e^- \bar{\nu}_e) = 10.82 \pm 0.02\%, \quad (25)$$

while the measured $Br(\tau^- \rightarrow \pi^- \nu_\tau)_{exp} = (10.91 \pm 0.07)\%$ [64]. In Fig. 2 we show the constraints on $m_H - \tan \beta$ from $\tau^- \rightarrow \pi^- \nu_\tau$. From Eq. 20 we can construct the NSI parameters defined in Ref [48] as $\varepsilon_{\tau\tau}^{ud(L)} \equiv \frac{m_u m_\tau}{m_H^2}$ and $\varepsilon_{\tau\tau}^{ud(R)} \equiv \frac{m_d m_\tau \tan^2 \beta}{m_H^2}$. We find that the constraints on the effective operator considered in this work are consistent with the one in Ref. [48]. Finally, we note that τ has a significant branching ratio

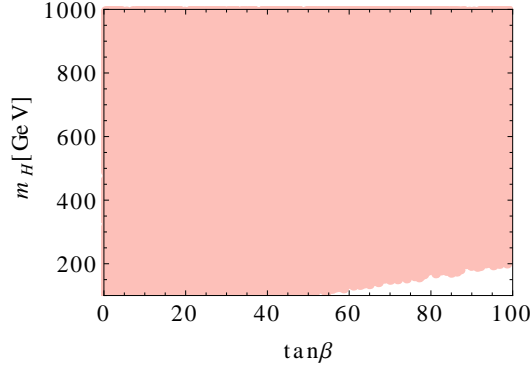


Figure 2: Constraint by $Br(\tau^- \rightarrow \pi^- \nu_\tau)$ at 95 % CL. The colored region is allowed.

to $\tau^- \rightarrow \rho^- \nu_\tau$ [64]. However, a charged Higgs cannot contribute to this decay, and hence there is no constraint on the charged Higgs couplings from this decay [50].

Keeping in mind the constraints from Fig. (2), we calculate the charged Higgs contribution to $\nu_\tau + n \rightarrow \tau^- + p$. The modified differential cross section for the reaction in Eq. (9) is

$$\frac{d\sigma_{SM+H}}{dt} = \frac{M^2 G_F^2 \cos^2 \theta_c}{8\pi E_\nu^2} \left[A_H + B_H \frac{(s-u)}{M^2} + C_{SM} \frac{(s-u)^2}{M^4} \right], \quad (26)$$

where $x_H = m_W^2/M_H^2$, $A_H = A_{SM} + 2x_H \text{Re}(A_H^I) + x_H^2 A_H^P$, and $B_H = B_{SM} + 2x_H \text{Re}(B_H^I)$. Superscripts I and P denote the SM-Higgs interference and pure Higgs contributions, respectively. The expressions for the quantities $A_H^{I,P}$ and B_H^I are given in the Appendix. The terms A_H^I and B_H^I are proportional to the tiny neutrino mass, and we will ignore them in our calculation. Note that this happens because we have chosen the couplings to be given by the 2HDM II. With general couplings of the charged Higgs, these interference terms will be present. The charged Higgs contribution relative to the SM $r_H^{23} = \frac{\sigma_H(\nu_\tau)}{\sigma_{SM}(\nu_\tau)}$ is proportional to t because of the dominant term $x_t G_P^2$, where $x_t = t/4M^2$ (see the Appendix for more details). Consequently, r_H^{23} is proportional to the incident neutrino energy (see Fig. (3)). The deviation δ_{23} is negative, as there is no interference with the SM; hence, the cross section for $\nu_\tau + n \rightarrow \tau^- + p$ is always larger than the SM cross section. This means that, if the actual θ_{23} is close to maximal, then experiments should measure θ_{23} larger than the maximal value in the presence of a charged Higgs contribution.

The differential cross section for the interaction $\bar{\nu}_\tau + p \rightarrow \tau^+ + n$ has the same form as Eq. 26 in the limit of a massless neutrino. The hadronic current in this case is the complex conjugate of the one in the Appendix. The ratio $r_H^{13} = \frac{\sigma_H(\bar{\nu}_\tau)}{\sigma_{SM}(\bar{\nu}_\tau)}$, as well as the deviation δ_{13} , is shown in Fig. 4. As θ_{13} is a small angle, large $\tan\beta$ and small charged Higgs mass are preferred to produce an observable deviation δ_{13} . For instance, we find $\delta_{13} \approx 1^\circ$ and $r_H^{13} \approx 30\%$ at $E_\nu = 8$ GeV, $M_H = 200$ GeV, and $\tan\beta = 100$.

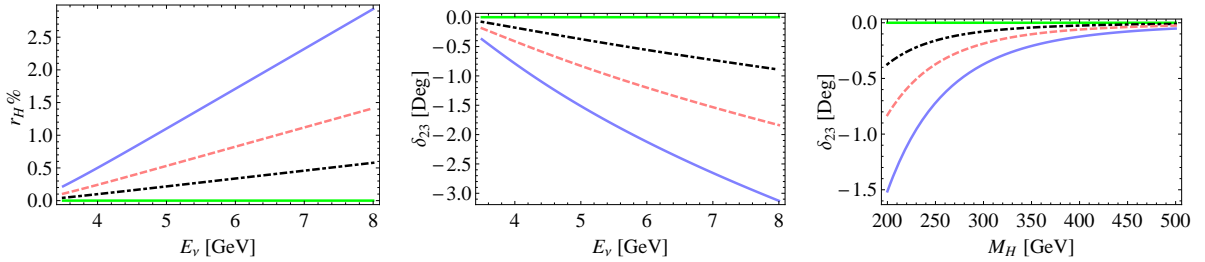


Figure 3: Variation of $r_H^{23}\%$ with E_ν and variation of δ_{23} with M_H and E_ν . The green line corresponds to the SM prediction. The black (dotdashed), pink (dashed), and blue (solid) lines correspond to $\tan\beta = 40, 50, 60$. The right figure is evaluated at $E_\nu = 5$ GeV, while the left figures are evaluated at $M_H = 200$ GeV. Here, we use the best-fit value $\theta_{23} = 42.8^\circ$ [53].

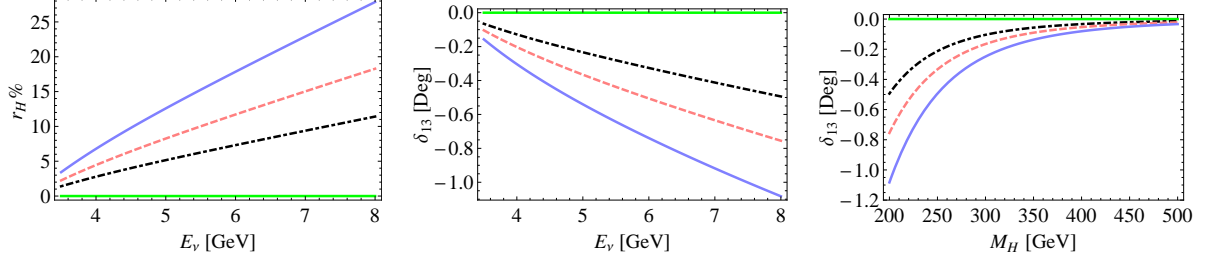


Figure 4: Variation of $r_H^{13\%}$ with E_ν and the variation of δ_{13} with M_H and E_ν . The green line corresponds to the SM prediction. The black (dotdashed), pink (dashed), and blue (solid) lines correspond to $\tan \beta = 80, 90, 100$. The right figure is evaluated at $E_\nu = 8$ GeV, while the left figures are evaluated at $M_H = 200$ GeV. Here, we use the inverted hierarchy value $\theta_{13} = 9.1^\circ$ [65].

5 Quasielastic neutrino scattering off free nucleon - W' model

Many extensions of the SM contain a W' gauge boson. We next consider modification to $\nu_\tau + n \rightarrow \tau^- + p$ and $\bar{\nu}_\tau + p \rightarrow \tau^+ + n$ in models with a W' . There are limits on the W' mass from direct searches to final states involving an electron and muon assuming SM couplings for the W' [64]. These limits generally do not apply to the W' coupling to ν_τ and τ which is relevant for our calculation.

The lowest dimension effective Lagrangian of W' interactions to the SM fermions has the form

$$\mathcal{L} = \frac{g}{\sqrt{2}} V_{f'f} \bar{f}' \gamma^\mu (g_L^{f'f} P_L + g_R^{f'f} P_R) f W'_\mu + h.c., \quad (27)$$

where f' and f refer to the fermions and $g_{L,R}^{f'f}$ are the left- and the right-handed couplings of the W' . For a SM-like W' boson, $g_L^{f'f} = 1$ and $g_R^{f'f} = 0$. We will assume $g_{L,R}^{f'f}$ to be real. Constraints on the couplings in Eq. (27) come from the hadronic τ decays. We will consider constraints from the decays $\tau^- \rightarrow \pi^- \nu_\tau$ and $\tau^- \rightarrow \rho^- \nu_\tau$.

The branching ratio for $\tau^- \rightarrow \pi^- \nu_\tau$ is

$$Br_{\tau^- \rightarrow \pi^- \nu_\tau}^{SM+W'} = Br_{\tau^- \rightarrow \pi^- \nu_\tau}^{SM} (1 + r_{W'}^\pi)^2, \quad (28)$$

where the W' contribution is

$$r_{W'}^\pi = x_{W'} g_L^{\tau\nu} (g_L^{ud} - g_R^{ud}), \quad (29)$$

and $x_{W'} = m_W^2/M_{W'}^2$. The branching ratio for the $\tau^- \rightarrow \rho^- \nu_\tau$ process is

$$Br_{\tau^- \rightarrow \rho^- \nu_\tau}^{SM+W'} = Br_{\tau^- \rightarrow \rho^- \nu_\tau}^{SM} (1 + r_{W'}^\rho)^2, \quad (30)$$

with the W' contribution

$$r_{W'}^\rho = x_{W'} g_L^{\tau\nu} (g_L^{ud} + g_R^{ud}). \quad (31)$$

The SM branching ratio is related to the decay rate as $Br_{\tau^- \rightarrow \rho^- \nu_\tau}^{SM} = \Gamma_{\tau^- \rightarrow \rho^- \nu_\tau}^{SM} / \Gamma_\tau$ with

$$\Gamma_{\tau^- \rightarrow \rho^- \nu_\tau}^{SM} = \frac{G_F^2}{16\pi} |V_{ud}|^2 f_\rho^2 m_\tau^3 \left(1 - \frac{m_\rho^2}{m_\tau^2}\right)^2 \left(1 + \frac{2m_\rho^2}{m_\tau^2}\right), \quad (32)$$

where $f_\rho = 223$ MeV [66]. Further, the SM branching ratio can also be expressed as [63]

$$Br_{\tau^- \rightarrow \rho^- \nu_\tau}^{SM} = 1.23 Br(\tau^- \rightarrow \nu_\tau e^- \bar{\nu}_e) = 21.92 \pm 0.05\%. \quad (33)$$

The measured branching ratio is $Br(\tau^- \rightarrow \rho^- \nu_\tau)_{exp} = (23.1 \pm 0.98)\%$ [64].

Figures 5 and 6 show the allowed regions for the W' couplings. The couplings are uniformly varied in the range $[-2, 2]$ and constrained by the measured $\tau^- \rightarrow \pi^- \nu_\tau$ and $\tau^- \rightarrow \rho^- \nu_\tau$ branching ratios with 1σ errors. From Eqs. (29, 31), the case with a pure left-handed W' coupling is allowed, as shown in Figs. (5, 6). The constraints on the effective operator are consistent with the one in Ref. [48]. From Eq. 27 the NSI parameter $\varepsilon_{\tau\tau}^{ud(L,R)}$ defined in Ref. [48] is given as $\varepsilon_{\tau\tau}^{ud(L,R)} \equiv g_L^{\tau\nu} g_{(L,R)}^{ud} (\frac{M_W}{M_{W'}})^2$.

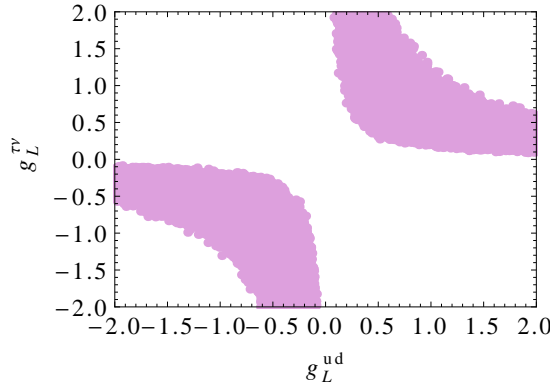


Figure 5: The constraints on the W' couplings without right-handed coupling at $M_{W'} = 500 - 1000$ GeV. The constraints are from $\tau^- \rightarrow \pi^- \nu_\tau$ and $\tau^- \rightarrow \rho^- \nu_\tau$ branching ratios. The errors in the branching ratios are varied within 1σ . The colored regions are allowed.

In the presence of the W' gauge boson, we can obtain the modified differential cross section for the reaction $\nu_\tau + n \rightarrow \tau^- + p$ as

$$\frac{d\sigma_{SM+W'}(\nu_\tau)}{dt} = \frac{M^2 G_F^2 \cos^2 \theta_c}{8\pi E_\nu^2} \left[A' + B' \frac{(s-u)}{M^2} + C' \frac{(s-u)^2}{M^4} \right], \quad (34)$$

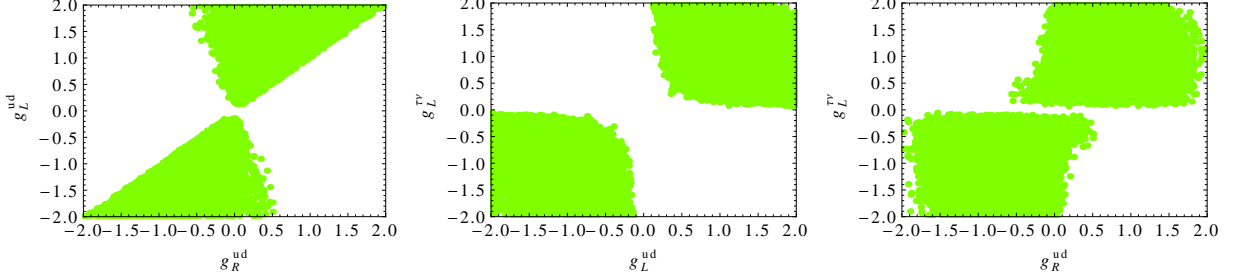


Figure 6: The constraints on the W' couplings with both left- and right-handed couplings at $M_{W'} = 500 - 1000$ GeV. The constraints are from $\tau^- \rightarrow \pi^- \nu_\tau$ and $\tau^- \rightarrow \rho^- \nu_\tau$ branching ratios. The errors in the branching ratios are varied within 1σ . The colored regions are allowed.

where the coefficients A', B', C' include both the SM and W' contributions. The expressions for these coefficients are given in the Appendix.

For a SM-like W' boson, with right-handed couplings ignored, the structure of the differential cross section is similar to the one in the SM case. Hence, the W' contribution relative to the SM $r_{W'}^{23} = \frac{\sigma_{W'}(\nu_\tau)}{\sigma_{SM}(\nu_\tau)}$ does not depend on the incident neutrino energy E_ν . We find $r_{W'}^{23} \sim 5\%$ at $M_{W'} = 500$ GeV from the hadronic tau decay constraints in Fig. (5). The variation of δ_{23} with the W' mass is shown in Fig. (7). In this case, δ_{23} is always negative and can reach up to -5° at $M_{W'} = 500$ GeV. Note that δ_{23} does not depend on E_ν either.

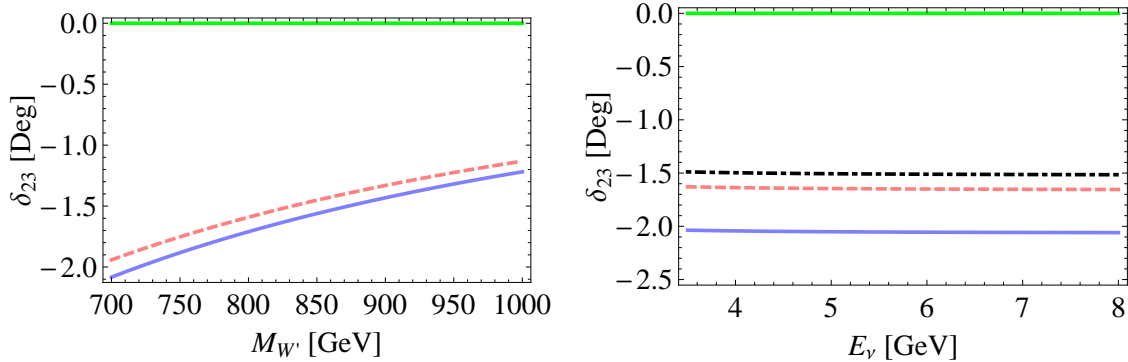


Figure 7: The left (right) panel illustrates the deviation δ_{23} with the W' mass (E_ν) when only left-handed W' couplings are present. The lines show predictions for some representative values of the W' couplings ($g_L^{\tau\nu_\tau}, g_L^{ud}$) taken from Fig. (5). The green line corresponds to the SM prediction. The blue (solid, lower) line in the left figure corresponds to (0.69, 0.89) at $E_\nu = 5$ GeV, and the blue (solid, lower) line in the right figure corresponds to (1.42, 0.22) at $M_{W'} = 500$ GeV. Here, we use the best-fit value $\theta_{23} = 42.8^\circ$ [53].

Next, we consider the right-handed couplings also. The variation of $r_{W'}^{23, \%}$ with $M_{W'}$ in this case is shown in Fig. (8). The $r_{W'}^{23, \%}$ values are mostly positive which, in turn, leads to δ_{23} being mostly negative. We find that $r_{W'}^{23, \%}$ depends slightly on the neutrino energy. The variation of δ_{23} with the W' mass and E_ν are shown in Fig. (9).

The W' contribution to the interaction $\bar{\nu}_\tau + p \rightarrow \tau^+ + n$ leads to the following differential cross section:

$$\frac{d\sigma_{SM+W'}(\bar{\nu}_\tau)}{dt} = \frac{M^2 G_F^2 \cos^2 \theta_c}{8\pi E_\nu^2} \left[A' - B' \frac{(s-u)}{M^2} + C' \frac{(s-u)^2}{M^4} \right]. \quad (35)$$

The differential cross section of the antineutrino scattering is relatively smaller than the corresponding one for the neutrino scattering because of the negative sign of the B coefficient. Thus, the value of the ratio $r_{W'}^{13} = \frac{\sigma_{W'}(\bar{\nu}_\tau)}{\sigma_{SM}(\bar{\nu}_\tau)}$ is smaller than the corresponding ratio, $r_{W'}^{23}$. Because of the smallness of θ_{13} and $r_{W'}^{13}$, the NP effect on the extraction of θ_{13} is small. Achieving large $r_{W'}^{13}$ within the constraints given in Fig. 6 is difficult in this model. This means the effect of the NP contribution in δ_{13} is very small and we do not plot the results of this calculations.

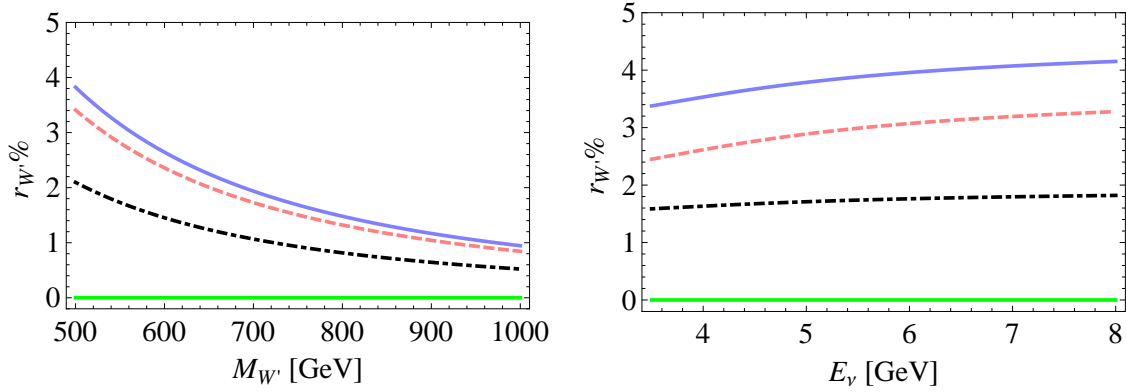


Figure 8: The left (right) panel illustrates the variation of $r_{W'}^{23, \%}$ in $\nu_\tau + n \rightarrow \tau^- + p$ scattering with the W' mass (E_ν) when both left- and right-handed W' couplings are present. The lines show predictions for some representative values of the W' couplings ($g_L^{\tau\nu\tau}, g_L^{ud}, g_R^{ud}$) taken from Fig. (6). The green line corresponds to the SM prediction. The blue (solid, upper) line in the left figure corresponds to $(-0.94, -1.13, -0.85)$ at $E_\nu = 5$ GeV, and the blue (solid, upper) line in the right figure corresponds to $(1.23, 0.84, 0.61)$ at $M_{W'} = 500$ GeV. Here, we use the best-fit value $\theta_{23} = 42.8^\circ$ [53].

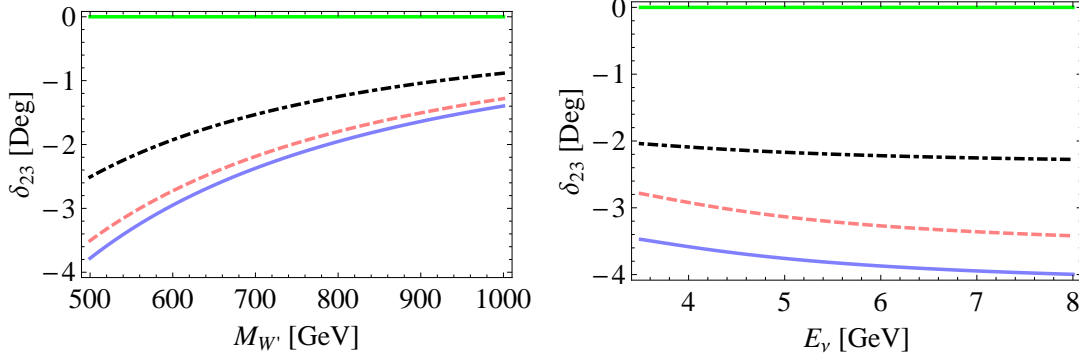


Figure 9: The left (right) panel illustrates the deviation δ_{23} with the W' mass (E_ν) when both the left- and right-handed W' couplings are present. The lines show predictions for some representative values of the W' couplings ($g_L^{\tau\nu_\tau}, g_L^{ud}, g_R^{ud}$) taken from Fig. (6). The green line corresponds to the SM prediction. The blue (solid, lower) line in the left figure corresponds to $(-0.94, -1.13, -0.85)$ at $E_\nu = 5$ GeV, and the blue (solid, lower) line in the right figure corresponds to $(1.23, 0.84, 0.61)$ at $M_{W'} = 500$ GeV. Here, we use the best-fit value $\theta_{23} = 42.8^\circ$ [53].

6 Conclusion

In this paper we calculated the effect of a charged Higgs and a W' contribution to $\nu_\tau + n \rightarrow \tau^- + p$ and $\bar{\nu}_\tau + p \rightarrow \tau^+ + n$ scattering. We constrained the parameters of both the models from $\tau^- \rightarrow \pi^- \nu_\tau$ and $\tau^- \rightarrow \rho^- \nu_\tau$ decays. Corrections to the SM contribution to $\nu_\tau + n \rightarrow \tau^- + p$ and $\bar{\nu}_\tau + p \rightarrow \tau^+ + n$ impact the extraction of the neutrino atmospheric mixing angles θ_{23} and θ_{13} , respectively. We found that the charged Higgs model can produce significant corrections to $\delta_{23,13}$ that measure the deviation of the actual $\theta_{23,13}$ from the $(\theta_{23,13})_{SM}$ angles which are extracted assuming the SM $\nu_\tau/\bar{\nu}_\tau$ scattering cross sections. The W' model effect generates a large deviation δ_{23} but negligibly small δ_{13} . As θ_{13} is smaller than θ_{23} larger NP in $\bar{\nu}_\tau + p \rightarrow \tau^+ + n$ is required to produce effects in δ_{13} similar in size to δ_{23} .

When a charged Higgs is involved, $\delta_{23,13}$ are negative. This is because there is no interference of the charged Higgs contribution with the SM contribution, for massless neutrinos, and so the cross sections for $\nu_\tau + n \rightarrow \tau^- + p$ and $\bar{\nu}_\tau + p \rightarrow \tau^+ + n$ are always larger than the SM cross sections. This means that experiments should measure $\theta_{23,13}$ larger than the present values in the presence of a charged Higgs contribution. In this case we also found that $\delta_{23,13}$ increase in magnitude with the neutrino energy. Hence, a possible sign of the charged Higgs effect would be a measurement of $\theta_{23,13}$ that shows an increase with increasing neutrino energy.

For the W' model we calculated a significant contribution to δ_{23} which can be both positive and negative, but is mostly negative. The deviation δ_{23} was found to be independent of the neutrino energy for a left-handed W' but neutrino energy

dependent when both left- and right-handed W' chiralities were present. A negligibly small deviation, δ_{13} , was found in the W' model because of the small value of θ_{13} .

We have presented in this paper a first estimation of the charged Higgs and W' effects in the extraction of θ_{23} and θ_{13} . We hope more detailed calculations including nuclear as well as detector effects, will be done to find out whether these new physics effects can be observed at present $\nu_\tau/\bar{\nu}_\tau$ appearance experiments and/or to motivate new experiments that can detect these effects.

Acknowledgements

We thank Sandip Pakvasa and Nita Sinha for useful discussions. This work was financially supported in part by the National Science Foundation under Grant No. NSF PHY-1068052.

Appendix

Hadronic form factors

The expressions for the vector and axial-vector hadronic currents in Eq. 44 are

$$\begin{aligned}\langle p(p')|V_\mu|n(p)\rangle &= \bar{u}_p(p')\left[\gamma_\mu F_1^V + \frac{i}{2M}\sigma_{\mu\nu}q^\nu F_2^V + \frac{q_\mu}{M}F_S\right]u_n(p), \\ -\langle p(p')|A_\mu|n(p)\rangle &= \bar{u}_p(p')\left[\gamma_\mu F_A + \frac{i}{2M}\sigma_{\mu\nu}q^\nu F_T + \frac{q_\mu}{M}F_P\right]\gamma_5 u_n(p).\end{aligned}\quad (36)$$

Here $q = p' - p$ and the form factors F_i are functions of $t = q^2$. The parametrizations of the axial-vector and pseudoscalar form factors are [57]

$$\begin{aligned}F_A(t) &= F_A(0)\left(1 - \frac{t}{M_A^2}\right)^{-2}, \\ F_P(t) &= \frac{2M^2 F_A(0)}{m_\pi^2 - t},\end{aligned}\quad (37)$$

where $F_A(0) = -1.2695$ is the axial coupling [64], m_π is the charged pion mass, and $M_A = 1.35$ GeV is the axial-vector mass [67]. The expression for $F_P(t)$ can be shown to be true at low energy, where the predictions of chiral perturbation theory are valid [68]. We have assumed the relation to hold at high t also. Note that $F_A(0)$ is sometimes replaced by $F_A(t)$, which gives similar results for $F_P(t)$ at low t but very different results at high t .

The Dirac and Pauli form factors $F_{1,2}^V$ are

$$F_1^V(t) = \frac{G_E(t) - x_t G_M(t)}{1 - x_t}, \quad F_2^V(t) = \frac{G_M(t) - G_E(t)}{1 - x_t}, \quad (38)$$

where $x_t = t/4M^2$ and

$$G_M = G_M^p - G_M^n, \quad G_E = G_E^p - G_E^n. \quad (39)$$

Here $G_E^{p,n}$ and $G_M^{p,n}$ are the electric and magnetic form factors of the proton and neutron, respectively. The simplest parametrizations of these form factors are given by the dipole approximation

$$G_E^p \approx G_D, \quad G_E^n \approx 0, \quad G_M^p \approx \mu_p G_D, \quad G_M^n \approx \mu_n G_D, \quad (40)$$

where $G_D = (1 - t/M_V^2)^{-2}$, $M_V = 0.843$ GeV is the vector mass, and $\mu_p(\mu_n)$ is the anomalous magnetic moment of the proton (neutron) [69].

In the presence of the charged Higgs, applying the equation of motion to the hadronic matrix elements for the scalar and pseudoscalar currents for the process $\nu_\tau + n \rightarrow \tau^- + p$ gives

$$\langle p(p') | \bar{u}(g_S^{u_i d_j} - g_P^{u_i d_j} \gamma_5) d | n(p) \rangle = V_{ud} \bar{p}(p_4) \left(g_S^{u_i d_j} G_S + g_P^{u_i d_j} G_P \gamma_5 \right) n(p_2), \quad (41)$$

or

$$\begin{aligned} \langle p(p') | \bar{u} d | n(p) \rangle &= \bar{p}(p_4) G_S n(p_2), \\ -\langle p(p') | \bar{u} \gamma_5 d | n(p) \rangle &= \bar{p}(p_4) G_P \gamma_5 n(p_2), \end{aligned} \quad (42)$$

where

$$\begin{aligned} G_S(t) &= r_N F_1^V(t), \quad \text{with } r_N = \frac{M_n - M_p}{(m_d - m_u)} \sim \mathcal{O}(1), \\ G_P(t) &= \frac{M[F_A(t) + 2x_t F_P(t)]}{\bar{m}_q}, \end{aligned} \quad (43)$$

with $\bar{m}_q = (m_u + m_d)/2$. In the W' model, the current has both $V \pm A$ structures. One has to calculate the matrix element,

$$\langle p(p') | J_\mu^+ | n(p) \rangle = V_{ud} \langle p(p') | \bar{u} (g_L^{ud} \gamma_\mu (1 - \gamma_5) + g_R^{ud} \gamma_\mu (1 + \gamma_5)) d | n(p) \rangle. \quad (44)$$

Kinematic details

The Mandelstam variables in terms of E_ν and the lepton energy E_l are

$$\begin{aligned} s &= M^2 + 2ME_\nu, \quad t = 2M(E_l - E_\nu), \\ s - u &= 4ME_\nu + t - m_l^2. \end{aligned} \quad (45)$$

Then t and E_l lie in the intervals

$$m_l^2 - 2E_\nu^{\text{cm}} (E_l^{\text{cm}} + p_l^{\text{cm}}) \leq t \leq m_l^2 - 2E_\nu^{\text{cm}} (E_l^{\text{cm}} - p_l^{\text{cm}}), \quad (46)$$

$$E_\nu + \frac{m_l^2 - 2E_\nu^{\text{cm}}(E_l^{\text{cm}} + p_l^{\text{cm}})}{2M} \leq E_l \leq E_\nu + \frac{m_l^2 - 2E_\nu^{\text{cm}}(E_l^{\text{cm}} - p_l^{\text{cm}})}{2M}, \quad (47)$$

where the energy and momentum of the lepton and the neutrino in the center of mass (cm) system are

$$\begin{aligned} E_\nu^{\text{cm}} &= \frac{(s - M^2)}{2\sqrt{s}}, \quad p_l^{\text{cm}} = \sqrt{(E_l^{\text{cm}})^2 - m_l^2}, \\ E_l^{\text{cm}} &= \frac{(s - M^2 + m_l^2)}{2\sqrt{s}}. \end{aligned} \quad (48)$$

The threshold neutrino energy to create the charged lepton partner is given by

$$E_{\nu_l}^{\text{th}} = \frac{(m_l + M_p)^2 - M_n^2}{2M_n}, \quad (49)$$

where m_l , M_p , M_n are the masses of the charged lepton, proton, and neutron, respectively. In our case, the threshold energy of the tau neutrino is $E_{\nu_\tau}^{\text{th}} = 3.45$ GeV.

The differential cross section in the laboratory frame is given by

$$\frac{d\sigma_{\text{tot}}(\nu_l)}{dt} = \frac{|\bar{\mathcal{M}}|^2}{64\pi E_\nu^2 M^2}. \quad (50)$$

The expressions for the coefficients f_{SM} ($f = A, B, C$) in the SM differential cross section [see Eq.(13)] are

$$\begin{aligned} A_{SM} &= 4(x_t - x_l) \left[(F_1^V)^2(1 + x_l + x_t) + (F_A)^2(-1 + x_l + x_t) + (F_2^V)^2(x_l + x_t^2 + x_t) \right. \\ &\quad \left. + 4F_P^2 x_l x_t + 2F_1^V F_2^V (x_l + 2x_t) + 4F_A F_P x_l \right], \\ B_{SM} &= 4x_t F_A (F_1^V + F_2^V), \\ C_{SM} &= \frac{(F_1^V)^2 + F_A^2 - x_t (F_2^V)^2}{4}, \end{aligned} \quad (51)$$

where $x_l = m_l^2/4M^2$.

The expressions for the quantities $A_H^{I,P}$ and B_H^I in the differential cross section in Eq. (26) are

$$\begin{aligned} A_H^I &= 2\sqrt{x_l}(x_t - x_l)g_P^{ud}(g_S^{l\nu_l} - g_P^{l\nu_l})G_P(F_A + 2F_P x_t), \\ B_H^I &= \frac{1}{2}\sqrt{x_l}g_S^{ud}(g_S^{l\nu_l} - g_P^{l\nu_l})G_S(F_1^V + F_2^V x_t), \\ A_H^P &= 2(x_t - x_l)(|g_S^{l\nu_l}|^2 + |g_P^{l\nu_l}|^2)(|g_P^{ud}|^2 G_P^2 x_t + |g_S^{ud}|^2 G_S^2 (x_t - 1)). \end{aligned} \quad (52)$$

For the 2HDM II model couplings, $g_{S,P}$ are given in Eq. (21). Note that the interference terms A_H^I and B_H^I vanish in this model.

The expressions for the quantities f' ($f = A, B, C$) in the differential cross section in Eq. (34) are

$$\begin{aligned}
A' &= 4(x_t - x_l) \left[(1 + r_{W'}^\rho)^2 \left((F_1^V)^2 (1 + x_l + x_t) + 2F_1^V F_2^V (x_l + 2x_t) + (F_2^V)^2 (x_l + x_t^2 + x_t) \right) \right. \\
&\quad \left. + (1 + r_{W'}^\pi)^2 \left((F_A)^2 (-1 + x_l + x_t) + 4F_A F_P x_l + 4F_P^2 x_l x_t \right) \right], \\
B' &= 4Re[(1 + r_{W'}^\rho)(1 + r_{W'}^{\pi*})] x_t F_A (F_1^V + F_2^V), \\
C' &= \frac{1}{4} \left[(1 + r_{W'}^\rho)^2 ((F_1^V)^2 - x_t (F_2^V)^2) + (1 + r_{W'}^\pi)^2 F_A^2 \right].
\end{aligned} \tag{53}$$

In the absence of W' contributions, the f' 's reduce to the respective SM results in Eq. 51.

References

- [1] L. Wolfenstein, Phys. Rev. D **17**, 2369 (1978).
- [2] S. P. Mikheev and A.Y. Smirnov, Sov.J.Nucl.Phys. 42 (1985) 913-917, Yad.Fiz. 42 (1985) 1441-1448
- [3] E. Roulet, Phys. Rev. D **44**, 935 (1991).
- [4] G. Brooijmans, hep-ph/9808498.
- [5] M. C. Gonzalez-Garcia, M. M. Guzzo, P. I. Krastev, H. Nunokawa, O. L. G. Peres, V. Pleitez, J. W. F. Valle and R. Zukanovich Funchal, Phys. Rev. Lett. **82**, 3202 (1999) [hep-ph/9809531].
- [6] M. M. Guzzo, A. Masiero and S. T. Petcov, Phys. Lett. B **260**, 154 (1991).
- [7] S. Bergmann, M. M. Guzzo, P. C. de Holanda, P. I. Krastev and H. Nunokawa, Phys. Rev. D **62**, 073001 (2000) [hep-ph/0004049].
- [8] M. M. Guzzo, H. Nunokawa, P. C. de Holanda and O. L. G. Peres, Phys. Rev. D **64**, 097301 (2001) [hep-ph/0012089].
- [9] M. Guzzo, P. C. de Holanda, M. Maltoni, H. Nunokawa, M. A. Tortola and J. W. F. Valle, Nucl. Phys. B **629**, 479 (2002) [hep-ph/0112310].
- [10] Y. Grossman, Phys. Lett. B **359**, 141 (1995) [hep-ph/9507344].
- [11] T. Ota and J. Sato, Phys. Lett. B **545**, 367 (2002) [hep-ph/0202145].

- [12] A. Friedland and C. Lunardini, Phys. Rev. D **72**, 053009 (2005) [hep-ph/0506143].
- [13] N. Kitazawa, H. Sugiyama and O. Yasuda, hep-ph/0606013.
- [14] A. Friedland and C. Lunardini, Phys. Rev. D **74**, 033012 (2006) [hep-ph/0606101].
- [15] M. Blennow, T. Ohlsson and J. Skrotzki, Phys. Lett. B **660**, 522 (2008) [hep-ph/0702059 [HEP-PH]].
- [16] A. Esteban-Pretel, J. W. F. Valle and P. Huber, Phys. Lett. B **668**, 197 (2008) [arXiv:0803.1790 [hep-ph]].
- [17] M. Blennow, D. Meloni, T. Ohlsson, F. Terranova and M. Westerberg, Eur. Phys. J. C **56**, 529 (2008) [arXiv:0804.2744 [hep-ph]].
- [18] M. C. Gonzalez-Garcia, Y. Grossman, A. Gusso and Y. Nir, Phys. Rev. D **64**, 096006 (2001) [hep-ph/0105159].
- [19] A. M. Gago, M. M. Guzzo, H. Nunokawa, W. J. C. Teves and R. Zukanovich Funchal, Phys. Rev. D **64**, 073003 (2001) [hep-ph/0105196].
- [20] P. Huber and J. W. F. Valle, Phys. Lett. B **523**, 151 (2001) [hep-ph/0108193].
- [21] T. Ota, J. Sato and N. -a. Yamashita, Phys. Rev. D **65**, 093015 (2002) [hep-ph/0112329].
- [22] M. Campanelli and A. Romanino, Phys. Rev. D **66**, 113001 (2002) [hep-ph/0207350].
- [23] M. Blennow, T. Ohlsson and W. Winter, Eur. Phys. J. C **49**, 1023 (2007) [hep-ph/0508175].
- [24] J. Kopp, M. Lindner and T. Ota, Phys. Rev. D **76**, 013001 (2007) [hep-ph/0702269 [HEP-PH]].
- [25] J. Kopp, M. Lindner, T. Ota and J. Sato, Phys. Rev. D **77**, 013007 (2008) [arXiv:0708.0152 [hep-ph]].
- [26] N. C. Ribeiro, H. Minakata, H. Nunokawa, S. Uchinami and R. Zukanovich-Funchal, JHEP **0712**, 002 (2007) [arXiv:0709.1980 [hep-ph]].
- [27] A. Bandyopadhyay *et al.* [ISS Physics Working Group Collaboration], Rept. Prog. Phys. **72**, 106201 (2009) [arXiv:0710.4947 [hep-ph]].
- [28] N. C. Ribeiro, H. Nunokawa, T. Kajita, S. Nakayama, P. Ko and H. Minakata, Phys. Rev. D **77**, 073007 (2008) [arXiv:0712.4314 [hep-ph]].

- [29] J. Kopp, T. Ota and W. Winter, Phys. Rev. D **78**, 053007 (2008) [arXiv:0804.2261 [hep-ph]].
- [30] M. Malinsky, T. Ohlsson and H. Zhang, Phys. Rev. D **79**, 011301 (2009) [arXiv:0811.3346 [hep-ph]].
- [31] A. M. Gago, H. Minakata, H. Nunokawa, S. Uchinami and R. Zukanovich Funchal, JHEP **1001**, 049 (2010) [arXiv:0904.3360 [hep-ph]].
- [32] A. Palazzo and J. W. F. Valle, Phys. Rev. D **80**, 091301 (2009) [arXiv:0909.1535 [hep-ph]]. A. Palazzo, Phys. Rev. D **83**, 101701 (2011) [arXiv:1101.3875 [hep-ph]].
- [33] K. Abe *et al.* [Super-Kamiokande Collaboration], arXiv:1206.0328 [hep-ex].
- [34] K. Abe *et al.* [Super-Kamiokande Collaboration], Phys. Rev. Lett. **97**, 171801 (2006) [hep-ex/0607059].
- [35] N. Agafonova *et al.* [OPERA Collaboration], arXiv:1107.2594 [hep-ex]. B. Won-sak [OPERA Collaboration], J. Phys. Conf. Ser. **335**, 012051 (2011).
- [36] K. Kodama *et al.* [DONuT Collaboration], Phys. Rev. D **78**, 052002 (2008) [arXiv:0711.0728 [hep-ex]].
- [37] Y. Abe *et al.* [DOUBLE-CHOOZ Collaboration], Phys. Rev. Lett. **108**, 131801 (2012) [arXiv:1112.6353 [hep-ex]].
- [38] F. P. An *et al.* [DAYA-BAY Collaboration], Phys. Rev. Lett. **108**, 171803 (2012) [arXiv:1203.1669 [hep-ex]].
- [39] J. K. Ahn *et al.* [RENO Collaboration], Phys. Rev. Lett. **108**, 191802 (2012) [arXiv:1204.0626 [hep-ex]].
- [40] K. Hagiwara, K. Mawatari and H. Yokoya, Nucl. Phys. B **668**, 364 (2003) [Erratum-ibid. B **701**, 405 (2004)] [hep-ph/0305324].
- [41] J. Conrad, A. de Gouvea, S. Shalgar and J. Spitz, Phys. Rev. D **82**, 093012 (2010) [arXiv:1008.2984 [hep-ph]].
- [42] A. Rashed, P. Sharma and A. Datta. [arXiv:1303.4332 [hep-ph]].
- [43] K. Ikado *et al.*, Phys. Rev. Lett. **97**, 251802 (2006) [arXiv:hep-ex/0604018].
- [44] J. P. Lees *et al.* [BaBar Collaboration], Phys. Rev. Lett. **109**, 101802 (2012) [arXiv:1205.5442 [hep-ex]].
- [45] A. Datta, M. Duraisamy and D. Ghosh, Phys. Rev. D **86**, 034027 (2012) [arXiv:1206.3760 [hep-ph]].

- [46] M. C. Gonzalez-Garcia, Y. Grossman, A. Gusso and Y. Nir, Phys. Rev. D **64**, 096006 (2001) [hep-ph/0105159].
- [47] D. Delepine, V. G. Macias, S. Khalil and G. Lopez Castro, Phys. Rev. D **79**, 093003 (2009) [arXiv:0901.1460 [hep-ph]].
- [48] C. Biggio, M. Blennow and E. Fernandez-Martinez, JHEP **0908**, 090 (2009) [arXiv:0907.0097 [hep-ph]].
- [49] U. Nierste, S. Trine and S. Westhoff, Phys. Rev. D **78**, 015006 (2008) [arXiv:0801.4938 [hep-ph]]. X. -G. He and G. Valencia, arXiv:1211.0348 [hep-ph].
- [50] K. Kiers, K. Little, A. Datta, D. London, M. Nagashima and A. Szykman, Phys. Rev. D **78**, 113008 (2008) [arXiv:0808.1707 [hep-ph]]; A. Datta, K. Kiers, D. London, P. J. O'Donnell and A. Szykman, Phys. Rev. D **75**, 074007 (2007) [Erratum-ibid. D **76**, 079902 (2007)] [hep-ph/0610162].
- [51] D. Meloni and M. Martini, arXiv:1203.3335 [hep-ph].
- [52] T. Teshima and T. Sakai, Analysis of atmospheric neutrino oscillations in three flavor neutrinos, Phys. Rev. D **62**, 113010 (2000) [hep-ph/0003038].
- [53] M. C. Gonzalez-Garcia, M. Maltoni and J. Salvado, JHEP **1004**, 056 (2010) [arXiv:1001.4524 [hep-ph]].
- [54] A. Donini, D. Meloni and P. Migliozi, Nucl. Phys. B **646**, 321 (2002) [hep-ph/0206034].
- [55] A. Upadhyay and M. Batra, arXiv:1112.0445 [hep-ph].
- [56] P. Huber, M. Lindner, M. Rolinec and W. Winter, Phys. Rev. D **74**, 073003 (2006) [hep-ph/0606119].
- [57] C. H. Llewellyn Smith, Phys. Rept. **3**, 261 (1972). S. K. Singh and E. Oset, Phys. Rev. C **48**, 1246 (1993). A. Strumia and F. Vissani, Phys. Lett. B **564**, 42 (2003) [astro-ph/0302055]. T. Gorrington and H. W. Fearing, Rev. Mod. Phys. **76**, 31 (2003) [nucl-th/0206039].
- [58] C. H. Llewellyn Smith, Phys. Rept. **3**, 261 (1972).
- [59] A. Strumia and F. Vissani, Phys. Lett. B **564**, 42 (2003) [astro-ph/0302055].
- [60] O. Deschamps, S. Descotes-Genon, S. Monteil, V. Niess, S. T'Jampens and V. Tisserand, Phys. Rev. D **82**, 073012 (2010) [arXiv:0907.5135 [hep-ph]].

- [61] See, e.g., R. A. Diaz, hep-ph/0212237, O. Deschamps, S. Descotes-Genon, S. Monteil, V. Niess, S. T'Jampens and V. Tisserand, Phys. Rev. D **82**, 073012 (2010) [arXiv:0907.5135 [hep-ph]], G. C. Branco, P. M. Ferreira, L. Lavoura, M. N. Rebelo, M. Sher and J. P. Silva, arXiv:1106.0034 [hep-ph].
- [62] M. Davier, A. Hocker and Z. Zhang, Rev. Mod. Phys. **78**, 1043 (2006) [hep-ph/0507078].
- [63] B. C. Barish, In *Stanford 1989, Proceedings, Study of tau, charm and J/psi physics* 113-126 and Caltech Pasadena - CALT-68-1580 (89,rec.Oct.) 14 p
- [64] K. Nakamura et al. (Particle Data Group), J. Phys. G 37, 075021 (2010) and 2011 partial update for the 2012 edition.
- [65] D. V. Forero, M. Tortola and J. W. F. Valle, arXiv:1205.4018 [hep-ph].
- [66] Z. G. Wang and S. L. Wan, Phys. Rev. C **76**, 025207 (2007) [hep-ph/0607135].
- [67] A. A. Aguilar-Arevalo et al. [MiniBooNE Collaboration], Phys. Rev. D 81 (2010) 092005.
- [68] T. Gorringer and H. W. Fearing, Rev. Mod. Phys. **76**, 31 (2003) [nucl-th/0206039].
- [69] K. S. Kuzmin, V. V. Lyubushkin and V. A. Naumov, Eur. Phys. J. C **54**, 517 (2008) [arXiv:0712.4384 [hep-ph]].